UNIVERSIDAD
NACIONAL
DE COLOMBIA

Petrologic features of mesoproterozoic lamprophyric dykes from Montevideo
(Piedra Alta terrane, South Uruguay)

Rossana Muzio[1], Natalia Martino[2], Elena Peel[1]
[1]Universidad de la República de Uruguay
[2]Dirección Nacional de Minería y Geología de Uruguay

ABSTRACT

Mafic dykes of lamprophyric affinity cropping out along the coastal area of Montevideo city are described. These dykes trend N75º-85º and crosscut 2.1 Ga Paleoproterozoic metamorphic units of the Rio de la Plata craton. They show mainly porphyritic textures with phlogopite and clinopyroxene macrocrysts in a groundmass composed of carbonates, phlogopite, augite, and feldspathoids. Ocellar structures filled with leucite, carbonates, and fibrous alkaline amphibole are present. The mineralogical assembly allows their classification as lamprophyres (minettes), but according to their chemical nature, they can be classified as alkaline lamprophyres. A crystallization age of 1.42 Ga by Ar-Ar method (on biotite/phlogopite) was obtained.

Rasgos petrológicos de los diques de lamprófidos mesoproterozoicos de Montevideo
(terreno Piedra Alta, sur de Uruguay)

RESUMEN

El presente trabajo describe a los diques máficos de afinidad lamprofídica presentes en la costa de la ciudad de Montevideo. Estos diques presentan tendencias estructurales N75º-85º con buzamientos verticales a subverticales y recortan a unidades metamórficas Paleoproterozoicas de 2.1 Ga del cratón del Rio de la Plata. Presentan texturas principalmente porfiríticas con macrocristales de flogopita y clinopiroxeno en una matriz compuesta por carbonatos, flogopita, augita y feldespatoides. Se observa, además, la presencia de estructuras ocelares rellenas por leucita, carbonatos y anfíbol fibroso alcalino. La textura y contenido mineralógico presente en estos diques permiten clasificarlos como lamprófidos (minettes), pero de acuerdo a su naturaleza química, pueden ser clasificados como lamprófidos alcalinos. Fue obtenida una edad de cristalización por método Ar-Ar (en biotita/flogopita) de 1.42 Ga.

Introduction

Lamprophyres comprise a set of uncommon hypoabissal mafic-ultramafic rocks usually of restricted occurrence as sills or dykes, occasionally as dyke swarms or stocks. They are usually linked to lamproite, kimberlite and carbonatite petrogenesis and to deep sublithospheric mantle melts. This group of rocks is characteristic of volatile-rich magmas, with fast ascent and emplacement at crustal levels during regional stages of lithospheric relaxation (Rock, 1987, 1991; Mitchell, 1994; Tappe et al., 2008). Alkaline magmatism is frequent in within-plate settings (Whalen et al., 1987; Bonin, 1996), associated with extensional processes. According to Rock (1991), chemical affinities define calk-alkaline, alkaline and ultramafic lamprophyres; the first usually being related to convergent settings, whereas the others two can be potentially related to large igneous provinces. Mostly, mafic dykes are prominent extensional structures and are helpful tools for paleogeography reconstructions as markers of former conjugate margins that were separated probably in relation to mantle plumes (e.g., Bleeker and Ernst, 2006; Ernst and Buchan, 2001a, b; Halls and Fahrig, 1987).

Mafic dykes have been formerly reported for the Rio de la Plata Craton (RPC), both for the Uruguayan shield and for the Tandilia belt in Argentina by Bossi et al., 1993; Mazzucchelli el al., 1995; Teixeira et al., 1999; Iacumin et al., 2001; and Teixeira et al., 2002; among other references. According to geochemical and isotopic studies, they correspond to a basaltic-andesite composition, with tholeiitic and calk-alkaline chemical affinity, and Paleo-Mesoproterozoic ages (Teixeira et al., 2013; Girardi et al., 2013).

Alkaline to sub-alkaline mafic magmatism has been found in southeast Uruguay, associated with the extensional events of the opening of the South Atlantic Ocean (Lustrino et al., 2005; Cernuschi et al., 2015).

The first references of lamprophyric dykes in Uruguay, that described the structural and petrographic features of mafic dykes located in the Montevideo coastal area, belong to Walther (1935; 1948). Later, regional studies on the crystalline basement of the RPC characterized these dykes as "mafic alkaline dykes", tentatively assigning them a Neoproterozoic age according to their field relationships, since they crosscut Paleoproterozoic units (Coronel and Oyhantçabal, 1988; Masquelin et al., 2003; Oyhantçabal et al., 2003; Pascale and Oyhantçabal, 2010).

Early reports of lamprophyres in the Tandilia basement (Argentina) correspond to the work of Quartino and Villar Fabre (1967), who described these rocks as possible deformed amphibolites. More recently, Dristas et al. (2013) carried out a petrological characterization on an ultramafic lamprophyre, also complemented by isotopic studies and K-Ar (on biotite/phlogopite) dating, yielding a minimum age of 1928 ± 54 Ma and a calk-alkaline nature.

Therefore, this paper is focused on the petrological characterization of a set of lamprophyric dykes in Uruguay and the first ^{40}Ar-^{39}Ar (on biotite/phlogopite) dating, in order to classify them and to constrain this magmatism in the context of the RPC.

Regional framework

Almeida et al. (1973) originally defined the Río de la Plata Craton (RPC), including under this term the "ancient cratonic areas" of the southernmost South American platform already amalgamated by the upper Proterozoic.

The RPC represents one of the major nuclei of Western Gondwana, surrounded by late Neoproterozoic–Cambrian orogenic belts (e.g., Almeida et al., 2000; Cingolani 2010; Rapela et al., 2011 and references therein). The main tectonic units exposed in the Uruguayan shield are represented by Piedra Alta (Bossi et al., 1993) and Nico Pérez (Bossi and Campal, 1992) terranes, which are separated by the Sarandí del Yí shear zone (Preciozzi et al., 1979). Both Piedra Alta and Nico Pérez terranes in Uruguay, together with Buenos Aires Complex (BAC) in Argentina (Marchese and Di Paola, 1975) and Taquarembó block in southern Brazil, constitute the RPC (Figure 1a), according to the original definition of Almeida et al. (1973). Recently, Oyhantçabal et al. (2011) redefined the RPC limits in Uruguay and excluded the Nico Pérez terrane and Taquarembó block from the craton, after new geochronological, isotopic and gravity data interpretations.

Most of the RPC consists of Paleoproterozoic crust over a large region of extension covered by Phanerozoic sediments; with characteristics of mature

Figure 1. (a) Main Rio de la Plata cratonic exposures (b) Location of the outcrop areas in the coastal zone of Montevideo city. References: PG - Punta Gorda site, 34°54´00"S – 56°4´53"W; RP - Rodó Park site, 34°55´11"S – 56°10´20"W; PAT = Piedra Alta Terrane, NPT = Nico Pérez Terrane, BAC = Buenos Aires Complex, SYSZ = Sarandí del Yí shear zone, Sierra Ballena shear zone, TB = Taquarembó Block.

continental crust (Cordani et al., 2000; Pankhurst et al., 2003; Peel and Preciozzi, 2006; Rapela et al., 2007). Remnants of Archean crust have been recognized by Hartmann et al. (2001) in Nico Pérez terrane (NPT).

The Piedra Alta terrane (PAT; Figure 1a) is comprised of low- to medium-degree metamorphic orogenic belts and plutonic suites (ca. 2.1 Ga), a layered mafic complex, late- to post-orogenic magmatism (1.9-2.3 Ga) and extensional magmatism (1.7 Ga) represented by the Florida mafic dyke swarm (Preciozzi et al., 1999; Bossi and Cingolani, 2009; Rapela et al., 2007; Sánchez Bettucci et al. 2010; Oyhantçabal et al., 2011; Hartmann et al., 2000). Peel and Preciozzi (2006) proposed that the PAT represents a juvenile Paleoproterozoic unit that has been stable since 1.7 Ga, without a record of the influence of Neoproterozoic orogenies. Similar features were also defined for the BAC (e.g., Bossi and Cingolani, 2009; Rapela et al., 2007; 2011). Halls et al. (2001) and Teixeira et al. (2013), reviewing the ENE-WSW trending Florida dyke swarm from PAT and the N-NW Tandil dykes in the BAC, obtained high-quality U-Pb (ID-TIMS in baddeleyite) ages of 1790 ± 5 Ma and 1589 ± 3 Ma, respectively. According to these results, Teixeira et al. (2013) suggested that both units underwent extensional regimes at the Paleo-Mesoproterozoic boundary.

The study area is located in the southern portion of the PAT, along the coastal margin of Montevideo city (Figure 2). This area consists of medium grade San José metamorphic belt (Bossi et al. 1993; Oyhantçabal et al. 2003), which includes the Montevideo Formation and the Punta Carretas Orthogneissic Unit. Both units are crosscut by pegmatitic and aplitic dykes and, by the mafic dykes of the present study.

The Montevideo Formation (Bossi 1965) is a supracrustal volcanic-sedimentary sequence metamorphosed under amphibolite facies conditions (Oyhantçabal et al. 2002; 2003). It is composed of concordant para-gneiss, para-amphibolites and mica schists, with an EW regional structural trend (Pascale 2013).

The Punta Carretas Orthogneissic Unit was defined by Oyhantçabal et al. (2003), who identified the orthogneiss as resulting from metamorphic recrystallization of calk-alkaline granitoids. It represents the most widespread unit of the crystalline basement in Montevideo, intercalated with rocks of the Montevideo Formation and associated granitoids (Pascale 2013). They present structural trends of N280º to N70º of light-gray to pinkish granolepidoblastic rocks, composed of oligoclase, quartz, biotite, epidote, muscovite, apatite and microcline, and strongly crosscut by pegmatitic and aplitic intrusions. The only radiogenic age available for this unit, by Rb-Sr whole rock method, yielded and age of 1990 ± 32 Ma (Cingolani et al. 1997).

Previous work, involving some petrographic and structural features of the lamprophyric dykes, inferred that they represent at least the last magmatic event affecting the Montevideo Formation (Pascale and Oyhantçabal 2010; Pascale 2013).

Analytical procedures

Seven rocks with minimal visible secondary alteration and corresponding to two different set of dykes from the coastal area were sampled, examined in thin section and prepared for lithogeochemical analyses. Three polished petrographic sections were also prepared at the Instituto de Ciencias Geológicas for SEM-EDS and BSE analyses. These analyses were developed with the JEOL 5900 - Low vacuum equipment at the Faculty of Sciences, Uruguay. Analytical techniques that are routine for this type of equipment as well as standard mineral spectra from Severin (2004) and Reed (2005) were used.

All the chemical data interpreted here as well as the location of the dykes are shown in Table 1. All samples were carefully cleaned, crushed and further pulverized using an agate mill at the Instituto de Ciencias Geológicas (Montevideo). Major and trace elements were analyzed by ACME-Bureau Veritas Laboratories (Vancouver, Canada) following the LF- 202 Litho-Research package methodology. Ba, Sr, Y, Sc, Zr, V, and Be were analyzed using inductively coupled plasma-atomic emission spectrometry (ICP-AES). Trace-elements (including REE) were determined by inductively coupled
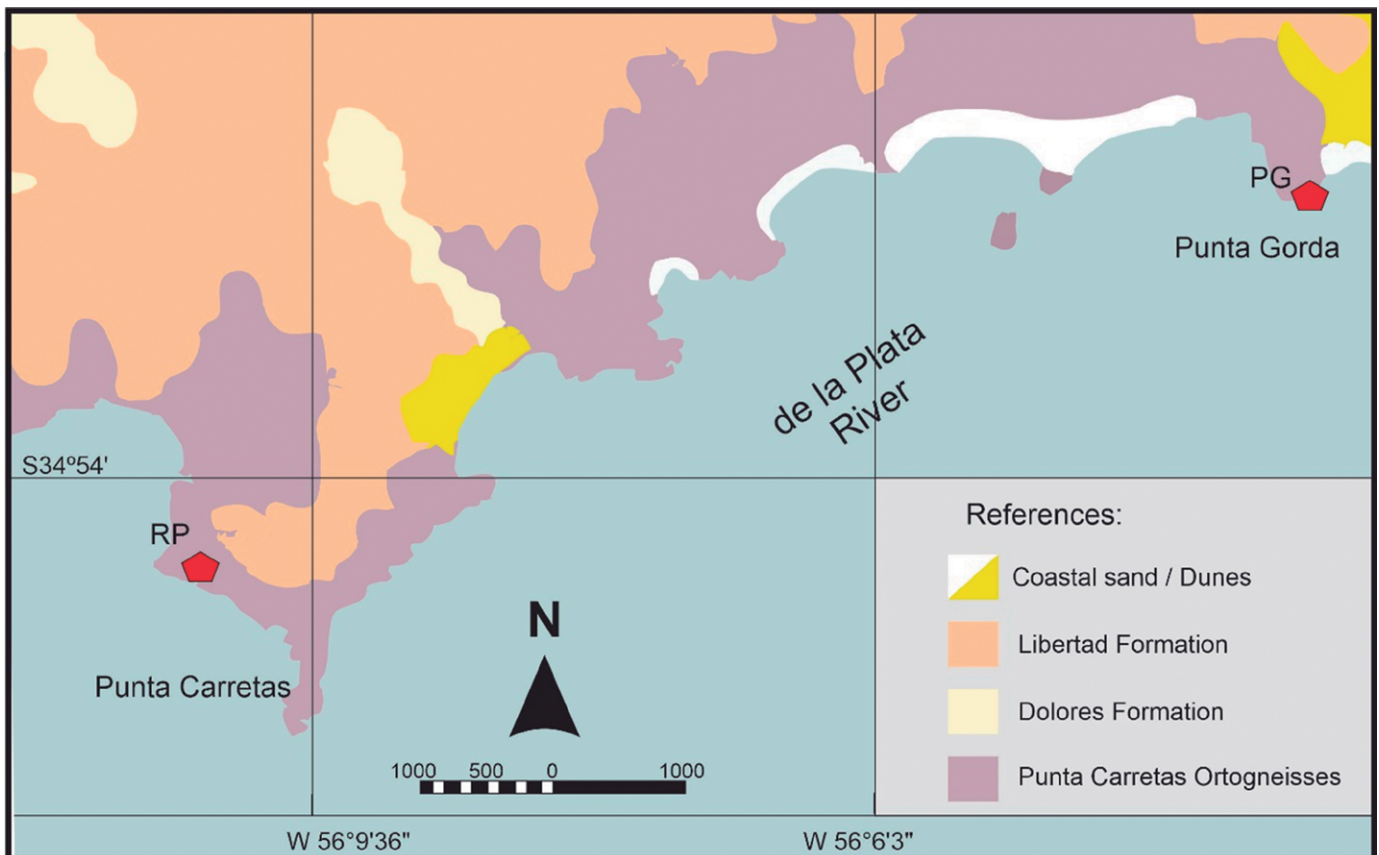

Figure 2. Geological sketch of the Montevideo coastal area (modified after Spoturno et al. 2004). References: Libertad Formation: Quaternary fine sediments; Dolores Formation: Quaternary wackes and mud sediments.

plasma-mass spectrometry (ICP-MS). The analytical protocol at the ACME Laboratory includes the analysis of reference materials (STD-DS10; STD-GS311-1; STD-GS910-4; STD- OREAS45EA; STD- SO-18 and STD SO-19).

The $^{40}Ar/^{39}Ar$ geochronology was carried out at the University of Nevada (Las Vegas), using the data reduction LabSPEC software written by B. Idleman (Lehigh University). Biotite crystals of one sample of a lamprohyre dyke (PG-01) were separated using conventional techniques and then irradiated at the U.S. Geological Survey TRIGA Reactor (Denver, Colorado) for 20 hours, along with the GA-1550 biotite standard together with CaF_2 and K-glass fragments. After a period of cooling, the irradiated sample was loaded for step heating in a Cu sample tray in a high vacuum extraction line and were fused using a 20 W CO_2 laser and measured using a Balzers electron multiplier mass spectrometer. The measured $(^{40}Ar/^{39}Ar)K$ values were 4.1 ($\pm$ 58.54%) x 10^{-3}. The Ca correction factors were $(^{36}Ar/^{37}Ar)Ca$ = 2.55 ($\pm$ 3.50%) x 10^{-4} and $(^{39}Ar/^{37}Ar)Ca$ = 6.97 ($\pm$ 3.69%) x 10^{-4}. The J factors were determined by fusion of 4-8 individual crystals of GA-1550 biotite neutron fluence monitors, giving a reproducibility of 0.3% to 0.8% at each standard position. The measured $^{40}Ar/^{36}Ar$ ratios were 282.36$\pm$1.41%; thus, a discrimination correction of 1.0467 (4 AMU) was applied to the measured isotope ratios. An age of 98.50 Ma (Spell and McDougall 2003) was used for the GA-1550 biotite fluence monitor to calculate the ages of the samples. The criterion followed to define a plateau age is the identification of three or more successive steps overlapping with an error at 2σ level that together comprise >50% of ^{39}Ar released. All analytical data are reported at the confidence level of 1σ (standard deviation) and shown in Table 2.

Petrographic features

Mafic dykes are gray to black, fine to medium grained, 0.3 to 2.0 meters width and tabular in shape. They often show irregular contacts with PAT units and are affected by two sets of NW and N-NW vertical to subvertical fractures. Sometimes they show an anastomosed pattern (Figure 3a), with sharp contacts and thin chilled margins (Figure 3d). No evidence of contact metamorphism has been found.

They are concordant with the regional foliation trend (N70º-N80º). Even the smaller dykes with widths of a few centimeters often intrude through lateral fractures with a NW direction. Double intrusion processes or "dyke in dyke" features are observed (Figure 3c), which has been well documented as a common process for lamprophyres worldwide (Rock 1987). They have porphyritic texture with increasing grain size toward the dyke center. Occasionally, the central zone is porphyritic and vesiculated, with biotite/pyroxene macrocrysts and globular structures.

These globular structures (*ocelli*; Phillpotts 1990) are almost spherical but frequently show coalescence, developing irregular shapes (Figure 3b). They vary in size between 0.1 cm to 1.5 cm, and they are filled mainly by carbonates, zeolites with halos of opaque minerals and arfvedsonite (Figure 3g).

Mafic and felsic xenoliths from the surrounding crystalline basement are frequent, represented by ortho-gneiss and amphibolite (Figures 3e and 3f).

Microscopically, rocks are porphyritic to glomeroporphyritic dykes, with biotite-phlogopite, augite-aegirine as main macrocrysts and with olivine and leucite subordinately; in a groundmass composed of alkaline feldspar (orthoclase), clinopyroxene, carbonate (dolomite), leucite, and opaque minerals (Figure 4a). The groundmass is very fine grained, showing an intergranular texture (between 50-100 μm). Feldspathoid glomeruli and carbonate patches are present within the groundmass (Figure 4b).

Globular structures (*ocelli*) are a common petrographic feature with radial halos of biotite-phlogopite and pale blue acicular amphibole, probably riebeckite/arfvedsonite (Figure 4c). Other *ocelli,* between 50-300 μm sized, are filled by carbonates, alkaline feldspar (orthoclase) and/or feldspathoid (leucite), (Figure 4d). According to these petrographic features they would correspond to Type 1 aggregates, as defined by Azbej et al. (2006). Opaque minerals vary approximately 5-10 modal %, they have subautomorph shapes and they are sometimes interstitially distributed in the groundmass.

SEM-EDS studies were developed to better characterize the mineral composition of the groundmass. The spectra obtained were compared to standard mineral spectra from Severin (2004) and Reed (2005) in order to identify part of the minerals of the dykes. Some of these representative minerals and their spectra are presented in Figure 5.

Figure 3. (a) Dyke showing anastomosed pattern at Punta Gorda (PG) site; (b) Ocelli with carbonate alteration rim; (c) dyke in dyke intrusion (PG site); (d) Detail of contacts with host rocks; (e) and (f) xenoliths from the surrounding crystalline basement represented mainly by ortho-gneiss and amphibolite; (g) ocelli filled mainly by carbonates, zeolites with halos of opaque minerals and arfvedsonite.
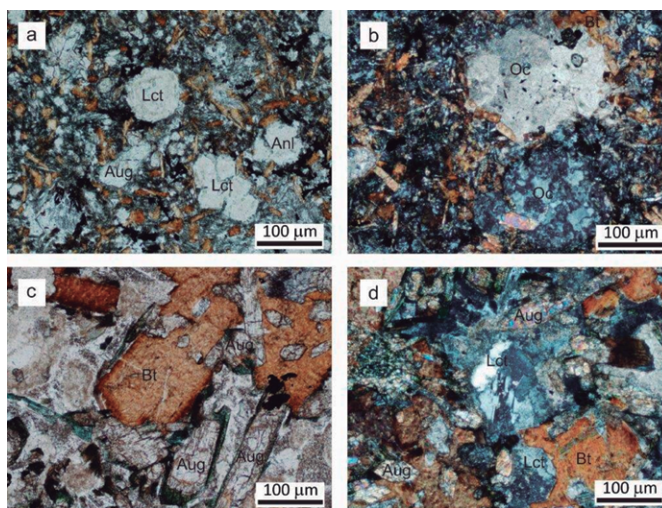

Figure 4. Photomicrographies under polarized microscope (crossed nicols), (a) Detail of the ocelli with leucite (Lct) and analcite (Anl) and phenocryst of augite (Aug); (b) Coalescent ocelli (Oc) filled with feldspathoids; (c) Augite (Aug) and biotite (Bt) phenocrysts; (d) Ocelli with carbonates (border) and leucite (Lct); groundmass with leucite, biotite, augite and carbonates.
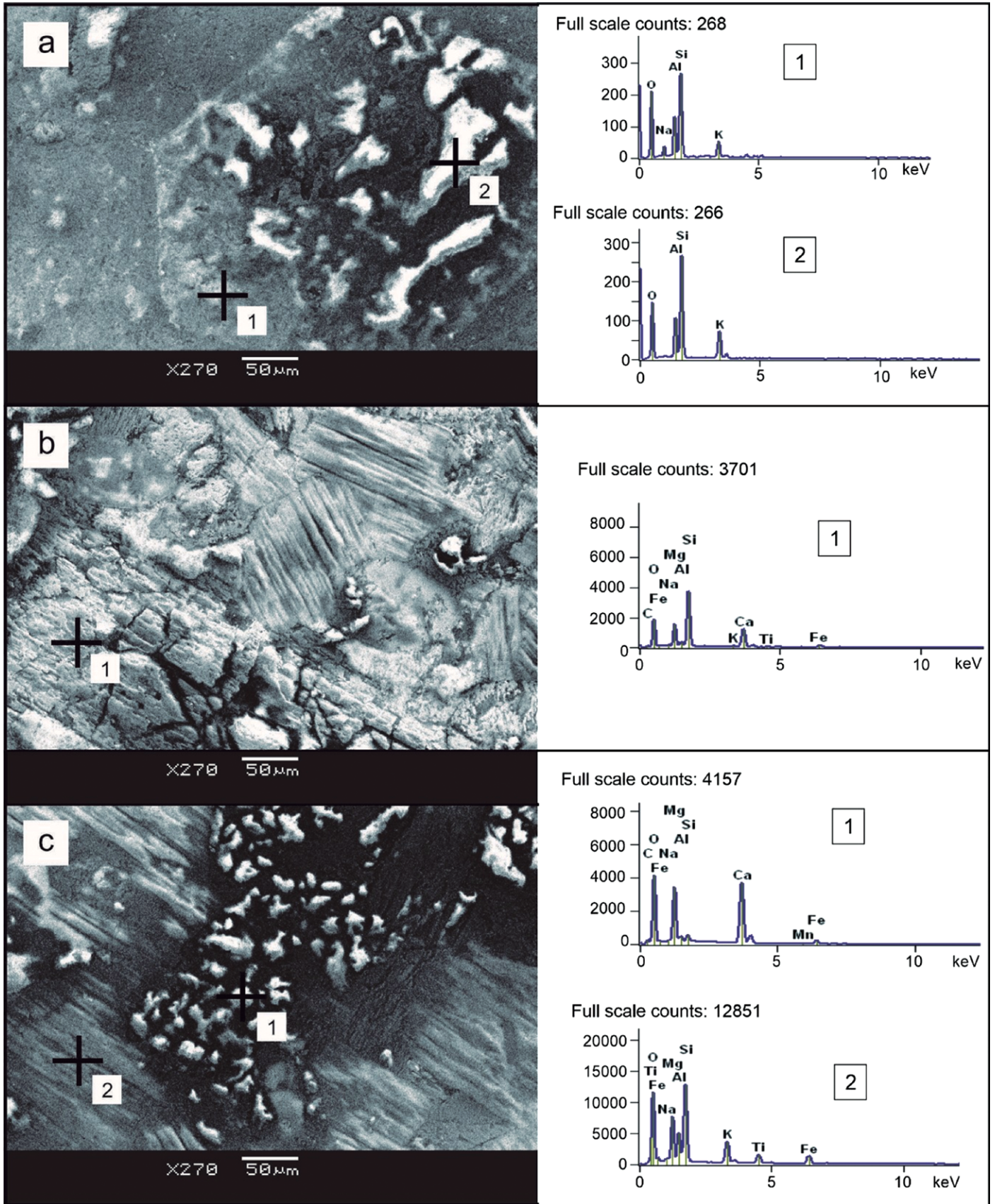
Figure 5. (a) BSE image with EDS spectra of leucite/nepheline crystal (sample PG-01); (b) BSE image of augite and phlogopite crystals (sample PG-04), EDS spectrum of augite. (c) BSE image of dolomite with spongy texture, showing high relief relative to the biotite and their respective EDS spectra (sample PG-01).

Lithogeochemistry

Analyses of seven samples and their locations are presented in Table 1. The dykes are low in SiO_2 (45.21%–51.43%), high in MgO (8.52%–11.08%), FeO_t (9.92%–10.42%), and TiO_2 (2.98-3.27%) and show exceptionally high values of K_2O ranging between 7.09-8.13%. They are enriched in incompatible elements, such as the HFSE, Zr (556-663 ppm), Nb (72-112 ppm) and Th (11-20 ppm) and the large ion lithophile elements, such as Ba (4486-5980 ppm), Sr (1017-2026 ppm) and Rb (129 -248 ppm).

According to the TAS diagram (Le Bas et al. 1986; Figure 6) the samples can be classified as phonotephrites/tephriphonolites. All the samples have total alkalis close to 10 wt% and K_2O/Na_2O ratios approximately 4, a relation that points to a possible ultrapotassic character/shoshonitic nature.
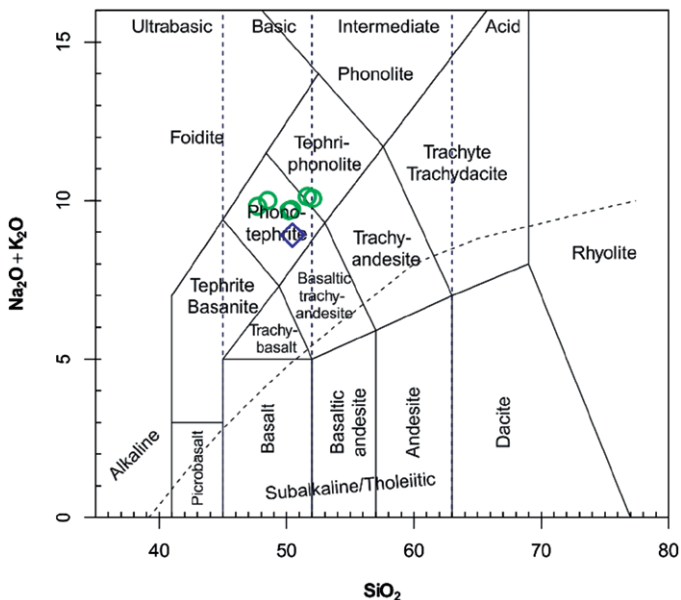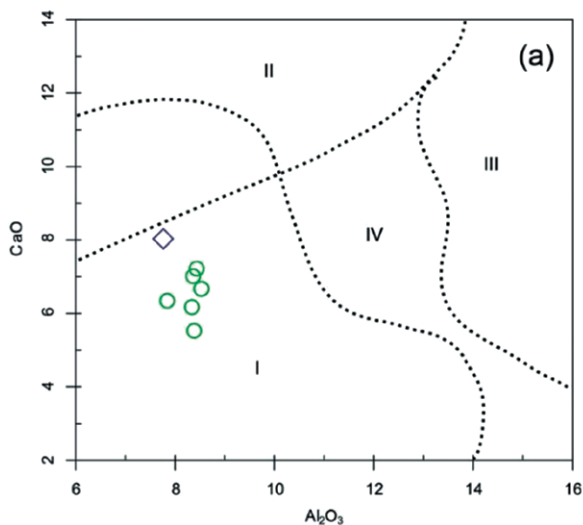

Figure 6. Classification diagrams (Le Bas et al. 1986). Symbols: ○ PG site; ◇ RP site.

Using the Al_2O_3 versus CaO classification diagram from Foley et al. (1987) and the K_2O-MgO-Al_2O_3 ternary diagram from Rock (1987), the samples can be classified as lamprophyres and, according to their alkali values the samples overlapped the fields lamprophyres/lamproites (Figure 7b).

As shown in Table 1, the samples have high alkali values (mean K_2O + Na_2O > 8, mostly close to 10 wt.%), with K_2O/Na_2O > 3. In order to constrain the alkaline affinity of the dykes and to discard a possible shoshonitic nature the K_2O – Na_2O diagram was used, showing as a result an ultrapotassic character for all the samples (Figure 8).
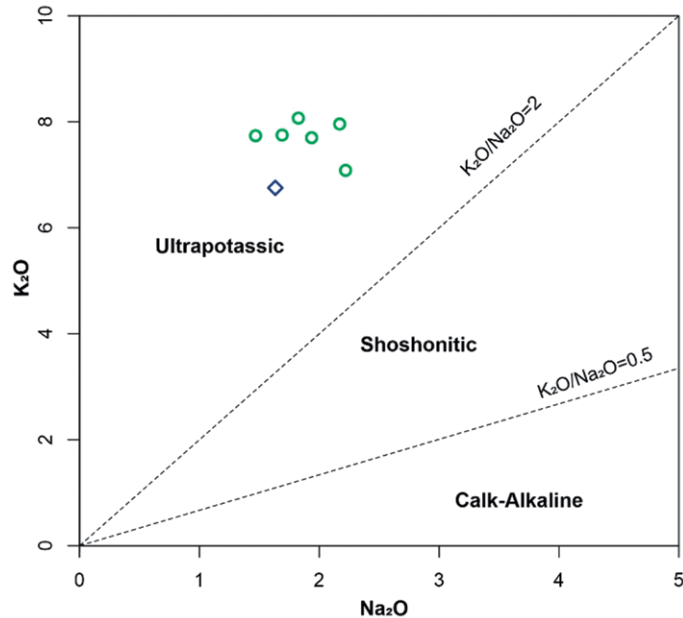

Figure 8. K_2O – Na_2O diagram, depicting the alkaline character (from Foley et al. 1987, after Turner et al. 1996). Symbols are the same as in Figure 6.

The REE patterns normalized to chondrite (Boynton 1984) are strongly fractionated, showing values from La to Lu between 110 – 600 ppm (Figure 9a), with different trends for the samples. In the primitive mantle-normalized multielement plot (Sun and McDonough 1989; Figure 9b), a significant enrichment in LILEs relative to HFSEs is observed, showing a steep pattern with through at U, Sr, and P and remarkable Ba and Nd positive spikes.
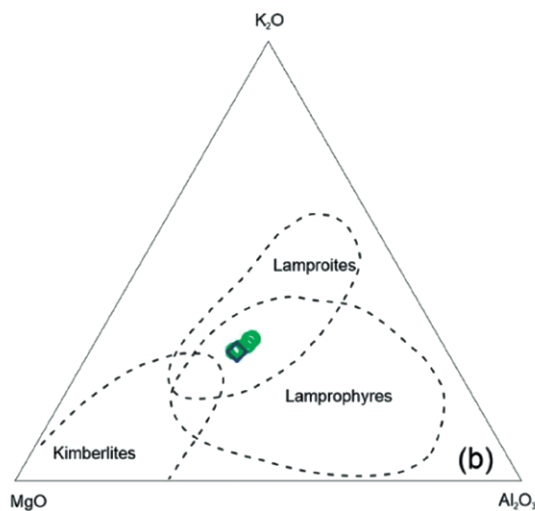

Figure 7. Classification diagrams for ultrapotassic rocks according to (a) Foley et al. (1987) and (b) Rock (1987). Symbols are the same as in Figure 6. References Fig. 7a: I – Lamproites; II – Kamafugites (low SiO_2, high Cao); III – Orogenic areas (high CaO and Al_2O_3) and IV – Transitional group.

Table 1. Geochemical data for the dykes from Punta Gorda (PG) and Rodó Park (RP) sites.

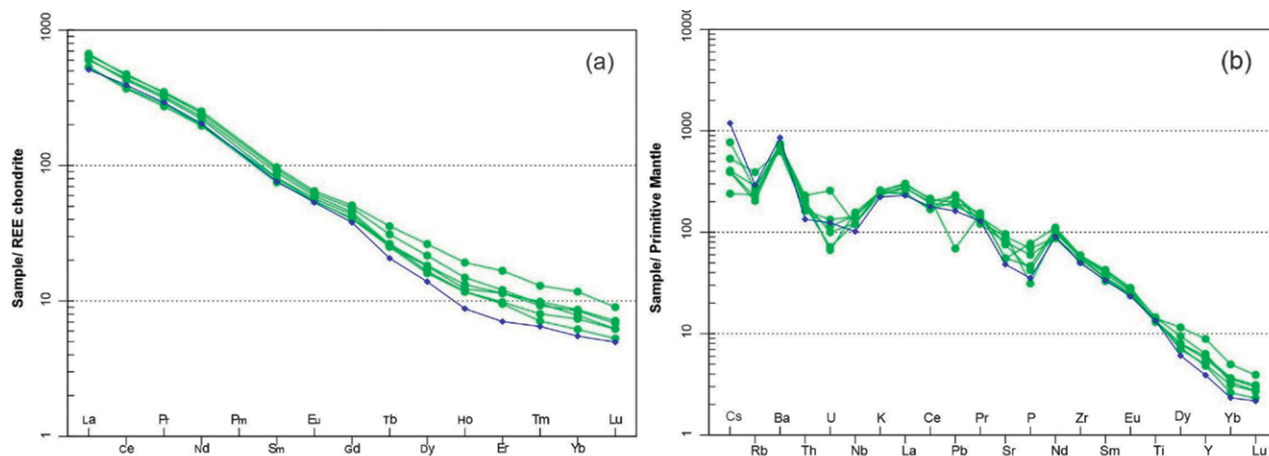| Sample	PG 01	PG 02	PG 03	PG 04	PG 05	PG 06	PR 02
Latitude	34º53'10,7"S	34º53'11.0"S	34º53'10,66"S	34º53'10,70"S	34º53'10,86"W	34º53'09,82"S	34º54'25,40"S
Longitude	56º04'52,2"W	56º04'52,12"W	56º04'51,65"W	56º04'51,77"W	56º04'52,12"W	56º04'51,30"W	56º10'08,90"W
SiO_2	49,37	47,03	49,67	44,61	46,58	45,32	46,83
Al_2O_3	8,38	7,84	8,34	8,43	8,53	8,36	7,76
Fe_2O_3	10,06	9,84	10,13	10,03	10,08	9,9	9,37
MgO	8,73	10,29	8,29	10,48	9,21	10,24	9,72
CaO	5,53	6,34	6,17	7,22	6,67	7,01	8,03
Na_2O	1,75	2,07	2,03	1,64	1,46	1,84	1,57
K_2O	7,8	7	7,71	7,54	7,53	7,5	6,7
K_2O/Na_2O	4,45	3,38	3,79	4,59	5,15	4,07	4,26
Total alkalis	9,55	9,07	9,74	9,18	8,99	9,34	8,27
TiO_2	3,14	2,89	3,08	2,9	2,96	2,82	2,91
P_2O_5	1,01	0,92	1,68	1,51	0,68	1,3	0,77
MnO	0,11	0,12	0,12	0,12	0,12	0,12	0,08
Cr_2O_3	0,047	0,049	0,049	0,046	0,039	0,046	0,057
LOI	2,9	4,4	1,6	4,3	4,9	4,4	5
Sum	98,89	98,86	98,9	98,87	98,78	98,91	99,5
Ba	5048	4867	5106	4399	5240	4486	5980
Be	8	9	8	2	5	3	3
Co	75,7	55,3	46,2	57,7	56	51	47,7
Cs	3,1	3,1	1,9	4,2	6,1	3,2	9,4
Ga	17,3	17,6	17,5	18,4	18,7	16,7	17,6
Hf	18,3	16,6	18,3	14,9	16,2	14,2	15,6
Nb	87,3	87,6	85,6	103,7	111,7	101,9	72,5
Rb	142,6	129,4	148,6	248	168,3	181,9	185,3
Sr	1170	1598,5	1160,3	1912,6	2026,5	1692,4	1017,6
Ta	4	4,2	4,8	5,1	5,3	5	4
Th	16,6	15,5	19,6	13,8	17,7	13,9	11,4
U	2,1	1,5	5,4	2,4	1,4	2,8	2,6
V	137	116	142	133	135	130	136
W	151	80,8	69,7	80,1	99,6	71,7	82,2
Zr	663,3	658,7	656,2	608	640,8	568,2	556,8
Y	28,7	21,9	40,4	27,1	22,5	25,6	17,7
La	201,9	186,8	207,1	165,4	189,6	163,2	158,7
Ce	382,1	354,4	374	303,1	344,7	299	317,2
Pr	41,87	39,65	42,53	34,8	38,44	33,39	35,59
Nd	145,4	137,6	150,8	119,2	132,1	118,1	122,3
Sm	18,23	17,28	18,93	15,66	15,81	14,64	14,91
Eu	4,58	4,39	4,76	4	4,18	4,03	3,93
Gd	12,59	11,74	13,17	10,59	11,29	10,46	9,84
Tb	1,47	1,23	1,69	1,25	1,19	1,2	0,98
Dy	6,97	5,34	8,48	5,87	5,17	5,84	4,47
Ho	1,07	0,84	1,38	0,95	0,84	0,88	0,63
Er	2,53	2	3,51	2,39	2,06	2,4	1,48
Tm	0,31	0,23	0,42	0,32	0,26	0,3	0,21
Yb	1,64	1,29	2,45	1,8	1,54	1,77	1,15
Lu	0,2	0,17	0,29	0,23	0,2	0,22	0,16
Pb	4,9	16,3	14	16,5	12,9	14,2	11,5
Ni	137,4	186,2	127,8	226,8	167,4	210,8	188

Figure 9. REE patterns and spider-diagrams, normalized according to (a) Chondrite (Boynton 1984); (b) Primitive mantle (Sun and Mc Donough 1989). Symbols are the same as in Figure 6.

The dykes have high Nb/Ta ratios, similar to the primitive mantle. Also, high Nb and Zr values with relatively low values of Hf and Y are commonly observed in alkaline rocks from within-plate settings (Green 1995).

$^{40}Ar/^{39}Ar$ results

The biotite-phlogopite analysis from the center of one dyke (Nº PG-01, site PG; Figure 2) produced relatively undisturbed spectra and a well-defined plateau age (Figure 10, Table 2) of 1425.40 ± 9.12 Ma (1σ). The plateau is defined by the release of at least 99% of ^{39}Ar gas in fifteen consecutive steps out of sixteen.

The anomalously young apparent age in the first low-temperature step yielded a general increasing trend for this spectrum. Minor disturbances also occur in high-temperature steps, suggesting degassing from high temperature resilient impurities. No statistically valid isochron was obtained.

Discussion

According to the petrographic features described previously, the analyzed dykes can be classified as lamprophyres. Based on the latter, the mineral assembly (biotite-phlogopite + augite ± aegirine augite ± altered olivine ± dolomite ± amphibole ± chlorite ± feldspars and feldspathoids, in the groundmass) and the high values of K_2O, P_2O_5 and Ba pointed to their classification as *minettes* (Rock 1991; Le Maitre et al. 2002). Although the presence of feldspathoids in *minette* type lamprophyres is not provided by the IUGS classification, it has been reported by several authors (e.g., Esperanza and Holloway 1987; Wallace and Carmichael, 1989; Bhowmick, 2000; Gupta 2015). In addition to the general mineralogical features, other chemical criteria can be taken into account to constrain their classification (Mitchell and Bergman, 1991).

In this sense, the dykes from Montevideo are not only ultrapotassic ($K_2O/Na_2O > 3$) but also peralkaline ($(K_2O+Na_2O)/Al_2O_3 > 1$) and perpotassic rocks

Table 2. Ar-Ar biotite analysis for the sample PG01. References: Biotite, 3.74 mg, J = 0.00497 ± 0.13%. 4 amu discrimination = 1.0467 ± 1.41%, 40/39K = 0.0041 ± 58.54%, 36/37Ca = 0.000255 ± 3.50%, 39/37Ca = 0.000697 ± 3.69%. Isotope beams in mV, r.l.s.d. = released, error in age includes J error; all errors 1 sigma. (36Ar through 40Ar are measured beam intensities, corrected for decay for the age calculations).

Step	T(°C)	t(min.)	^{36}Ar	^{37}Ar	^{38}Ar	^{39}Ar	^{40}Ar	$\%^{40}Ar^*$	$\%^{39}Ar$ rlsd	Ca/K	$^{40}Ar^*/^{39}ArK$	Age(Ma)	1s.d.
1	660	12	0,701	0,570	0,383	9,490	2176,69	91,3	1,2	3,9904378	211,358746	1295,44	17,28
2	730	12	0,167	0,655	0,378	21,589	5206,83	99,3	2,8	2,0144702	241,890087	1424,24	17,42
3	770	12	0,153	0,137	0,570	35,889	8766,62	99,6	4,7	0,2533259	245,814014	1440,14	17,56
4	800	12	0,134	0,057	0,753	48,149	11716,88	99,8	6,3	0,078557	245,263035	1437,92	17,51
5	830	12	0,090	0,054	0,736	52,424	12694,65	99,9	6,8	0,0683533	244,355218	1434,25	17,43
6	870	12	0,080	0,048	0,926	58,059	14098,14	99,9	7,6	0,0548613	245,123479	1437,35	17,53
7	910	12	0,063	0,068	0,858	57,968	14174,76	99,9	7,6	0,0780717	246,930930	1444,64	17,54
8	950	12	0,077	0,102	0,854	54,603	13223,94	99,9	7,1	0,1239616	244,475970	1434,75	17,44
9	990	12	0,076	0,128	0,775	47,539	11555,55	99,9	6,2	0,1786778	245,340750	1438,23	17,47
10	1030	12	0,051	0,086	0,561	34,622	8244,25	100,0	4,5	0,1648371	240,389997	1418,12	17,30
11	1060	12	0,047	0,076	0,451	25,858	6133,56	100,0	3,4	0,1950434	239,393167	1414,04	17,27
12	1090	12	0,052	0,083	0,406	22,437	5263,66	100,0	2,9	0,2454893	236,639139	1402,73	17,17
13	1120	12	0,055	0,125	0,482	25,191	5923,03	99,9	3,3	0,3293025	237,205720	1405,06	17,22
14	1160	12	0,097	0,486	1,110	64,621	15221,67	99,9	8,4	0,4991319	234,165292	1392,51	17,10
15	1210	12	0,095	0,593	1,918	121,984	29396,48	100,0	15,9	0,3226126	243,445057	1430,56	17,41
16	1400	12	0,103	0,411	1,294	86,712	20893,79	100,0	11,3	0,314551	243,308533	1430,00	17,40

Cumulative % ^{39}Ar rlsd =   100,0   Total gas age =   1426,19   8,64

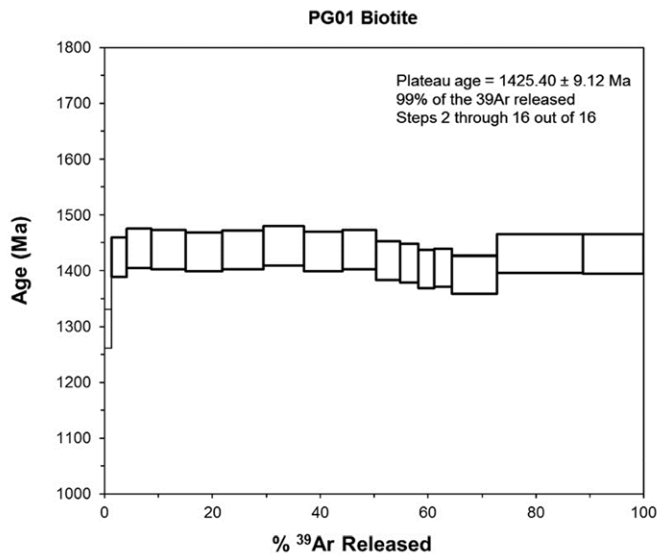Plateau age =   1425,40   9,12

(steps 2-16)

Figure 10. Step-heating spectrum obtained from biotite (sample PG01). Apparent age is given at 1σ.

$(K_2O/Al_2O_3 > 1)$, with CaO and $Fe_2O_{3t} \leq 10$ wt. % and a high Ba (>5.000 ppm), TiO_2 (~3 wt. %), Zr (~650 ppm) and Sr (~1500 ppm). All these are typical characteristics of lamproites according to Foley et al. (1987) and Le Maitre et al. (2002). Nevertheless, the typical lamproite mg# values are higher than 70, and the La content is higher than 200 ppm whereas in the studied dykes they are between 62-67 and approximately 182, respectively. The dykes present a mean value of 3.7 for the Nb/Y ratio, which characterizes them as alkaline (Winchester and Floyd, 1977). Alkaline lamprophyres usually have Cr, Co and Ni contents of 97, 38 and 65 ppm, respectively. In contrast, the lamprophyric dykes of Montevideo have these values of approximately 480, 56 and 172 ppm, close to those representatives of ultrapotassic lamprophyres (Mitchell and Bergman, 1991).

All dykes present high K/Ti and $(La/Sm)_N$ ratios (>2.3 and > 2.6, respectively) that are commonly related to enriched mantle sources (Mahoney et al. 2002). The mg# (62-67) suggests a mantle source for these dykes from values of Sc (15-16 ppm), Cr (420-520 ppm), Co (47-75 ppm) and Ni (143-239 ppm) (Rhodes, 1981).

Alkaline magmatism is frequent in within-plate environments, related to extensional processes (Whalen et al. 1987) and is characterized by high concentrations of HFSE and low values of LILE. Alkaline rocks showing strong enrichment in LILE and LREE are commonly associated with anorogenic or post-orogenic settings (Plá et al., 2011).

Alkaline ultrapotassic magma shows high incompatible element content regardless of the tectonic environment supporting an origin by partial melting of lherzolites (low rates <1%) from an enriched mantle source (Lloyd et al. 1985; Foley 1992; Foley and Peccerillo 1992; Ionov et al. 1997). Furthermore, high concentrations of LREE have been observed for other ultrapotassic within plate rocks, such as lamprophyres and lamproites as well as post-collisional lamprophyres like *minettes* (Foley 1992; Gibson et al. 1992). The high concentrations of Y and Zr, and relatively lower concentrations of Hf, Nb, Ta and HFSE are consistent with a within plate environment (Foley and Peccerillo, 1992). The Nb/U ratios for lower and upper crust are 21 and 9, respectively; rocks affected by crustal contamination present Nb/U values between 9 and 40 ppm (Gregoire et al., 2000). The dyke mean values of 43 ppm suggest that crustal contamination during the magmatic ascent/ emplacement is not obvious.

Several authors (e.g., Masquelin et al. 2003, Oyhantçabal et al., 2003, Pascale and Oyhantçabal, 2010) have attributed a Cambrian age to these dykes because other mafic dykes located to the North of Montevideo city crosscut the La Paz granite (585 ± 4 Ma, Cingolani et al. 2012). Martino (2017) analyzed these dykes and found that they correspond to lamprophyres of calk-alkaline affinity, and according to their petrographic features they were classified as espessartites. Interesting features that support their contemporaneity of emplacement with the La Paz granite are evidence of magma mingling processes. Therefore, these calk-alkaline lamprophyres are clearly different and

later than the dykes discussed in this paper. Mafic dykes of Mesoproterozoic age have been mentioned for the RPC, but in general, with different mineralogy and/or chemical affinity (Girardi et al. 2013; Teixeira et al. 2013; Dristas et al. 2013, among others). An interesting fact reported by these authors is that according to the isotopic data from the Tandil dykes, an enriched original source could be a characteristic feature of the mantle of the Rio de la Plata Craton in Paleoproterozoic time. Lamprophyric dykes were only reported by Dristas et al. (2013), with a minimum age of 1.92 ± 54 Ga obtained by the K-Ar method on phlogopites. Teixeira et al. (2013) proposed the idea that the Columbia supercontinent started a major break up at 1.59 Ga, based on geochronological and paleomagnetic data. Therefore, the emplacement of the lamprophyric dykes studied in this paper may be related to the initial stages of a later major extensional event.

Conclusions

• The lamprophyric dykes from Montevideo, with variable structural trend between N75º-N85º, have porphyritic texture with mainly phlogopite phenocrysts and a groundmass composed of biotite-phlogopite + augite – aegirine augite ± altered olivine ± dolomite ± amphibole ± chlorite ± feldspars and feldspathoids. Ocellar structures with carbonate, zeolites, leucite and fibrous alkaline amphibole are present.

• They are chemically ultrapotassic dykes (K2O/Na2O > 3), with peralkaline $(K_2O+Na_2O)/Al_2O_3 > 1)$ and perpotassic nature $(K_2O/Al_2O_3 > 1)$, with CaO and $Fe_2O_{3t} \leq 10$ wt. %, very high Ba (>5.000 ppm), TiO_2 (~3 wt. %), Zr (~650 ppm), and Sr (~1500 ppm), mg# approximately 63-67 and they are highly enriched in LILE in relation to primitive mantle.

• According to the mineralogical criteria established by the IUGS the dykes can be classified as *minettes* (lamprophyres) and from a chemical point of view as alkaline/ ultrapotassic lamprophyres.

• The chemical features point to a deep/enriched mantle source for the origin of this magma related to a within-plate tectonic setting.

• The crystallization age of 1.42 Ga determined by the Ar/Ar method on biotite (phlogopite), points to an extensional event for the Rio de la Plata craton at that time.

References

Almeida, F. F. M., Amaral, G., Cordani, U. G. & Kawashita, K. (1973). The Precambrian evolution of the South American cratonic margin South of the Amazon River. In: Nairm A.E. & Stehli F.G. (Eds.) *The ocean basins and margins, 1* (The South Atlantic), Plenum Press, New York, 441-446.

Almeida, F. F. M., Brito Neves, B. B. & Carneiro, C. D. (2000). The origin and evolution of the South American Platform. *Earth-Science Reviews*, 50, 77–111. https://doi.org/10.1016/S0012-8252(99)00072-0

Azbej, T., Szabo, C., Bodnar, R. & Dobosi, G. (2006). Genesis of carbonate aggregates in lamprophyres from the northeastern Transdanubian Central Range, Hungary: Magmatic or hydrothermal origin? *Mineralogy and Petrology*, 88, 479–497. https://doi.org/10.1007/s00710-006-0123-y

Bhowmick, S. K. (2000). Ultrapotassic rocks along late ductile shear zones from Eastern Ghats belt, India. *Gondwana Research*, 3, 55-63. https://doi.org/10.1016/S1342-937X(05)70057-5

Bleeker, W. & Ernst, R. (2006). Short-lived mantle generated magmatic events and their dyke swarms: The key unlocking Earth's paleogeographic record back to 2.6 Ga. In: Hanski, S., Mertanen, T., Rämö, T.& Vuollo, J. (Eds.) *Dyke Swarms — The Markers of Crustal Evolution*. London, 23–26.

Bonin, B. (1996). A-type granite ring complexes: mantle origin through crustal filters and the anorthosite–rapakivi magmatism connection. In:

Demaiffe, D. (Ed.) *Petrology and geochemistry of magmatic suites of rocks in the continental and oceanic crusts*. Bruxelles, 201-217.

Bossi, J. (1965). *Geología del Uruguay*. Departamento de Publicaciones de la Universidad de la República, Montevideo, 460 pp.

Bossi, J. & Campal, N. (1992). *Magmatismo y tectónica transcurrente durante el Paleozoico Inferior en Uruguay*. In: De Gutiérrez Marco, J., Saavedra, J., & Rábano, I. (Editors). Simposio Internacional del Paleozoico Inferior Latinoamericano, Actas, I. Salamanca, España, 343-356.

Bossi, J., & Cingolani, C. (2009). *Extension and general evolution of the Río de la Plata Craton*. In: Gaucher, C., Sial, A. N., Halverson, G. P. & Frimmel, H. E. (Eds) Neoproterozoic–Cambrian Tectonics, Global Change and Evolution: A Focus on Southwestern Gondwana. Elsevier, Developments in Precambrian Geology, 16, 73–85.

Bossi, J., Preciozzi, F. & Campal, N. (1993). Predevoniano en el Uruguay. Tomo I-Terreno Piedra Alta. Dirección Nacional de Minería y Geología, Montevideo, 50 pp.

Boynton, W. (1984). *Geochemistry of the rare earth elements: meteorite studies*. In: Henderson, H. (Ed.). Rare earth element geochemistry. Elsevier Science, Amsterdam, 63-114.

Cernuschi, F., Dilles, J. H., Kent, J. R., Schroer, G., Raab, A. K., Conti, B., & Muzio, R. (2015). Geology, geochemistry and geochronology of the Cretaceous Lascano East intrusive complex and magmatic evolution of the Laguna Merín basin, Uruguay. *Gondwana Research*, 28, 837–857. DOI:10.1016/j.gr.2014.07.007

Cingolani, C. A. (2010). The Tandilia System of Argentina as a southern extension of the Rio de la Plata craton: an overview. *International Journal of Earth Sciences*, 100(2), 221–242. DOI:10.1007/s00531-010-0611-5

Cingolani, C., Basei, M., Bossi, J., Piñeyro, D. & Uriz, N. (2012). *U-Pb (LA-ICP-MS) zircon age of the La Paz Granite (Pando Belt, Uruguay): an Upper Neoproterozoic magmatic event in the Río de la Plata Craton*. VIII South American Symposium on Isotope Geology, Medellín, Colombia, Abstracts (CD-ROM), 139.

Cingolani, C., Varela, R., Dalla Salda, L., Bossi, J., Campal, N., Ferrando, L., Piñeiro, D., & Schipilov, A. (1997). *Rb/Sr geocronology from the Río de la Plata Craton of Uruguay*. I South American Symposium on Isotope Geology, Campos do Jordão, Brazil, Abstracts.

Cordani, U., Sato, K., Teixeira, W., Tassinari, C. & Basei, M. A. S. (2000). Crustal evolution of the South American platform. In: Cordani, U. G., Milani, E. J., Thomaz-Filho, A. & Campos, D. A. (Eds.) Tectonic Evolution of South America, Finep, Brazil, 19–40.

Coronel, N., & Oyhantçabal, P. (1988). *Carta geológica del Uruguay a escala 1/100.000-fotoplano J-28 Pando*. Dirección Nacional de Minería y Geología-Facultad de Agronomía-Facultad de Ciencias, Montevideo, Uruguay.

Dristas, J., Martínez, J., Massonne, H., & Pimentel, M. (2013). Mineralogical and geochemical characterization of a rare ultramafic lamprophyre in the Tandilia belt basement, Río de la Plata Craton, Argentina. *Journal of South American Earth Sciences,* 43, 46-61. https://doi.org/10.1016/j.jsames.2013.01.002

Esperanza, S., & Holloway, J. (1987). On the origin of some mica-lamprophyres: experimental evidence from a mafic minette. *Contributions to Mineralogy and Petrology,* 95, 207-216. https://doi.org/10.1007/BF00381270

Ernst, R. E., & Buchan, K. L. (2001a). *The use of mafic dike swarms in identifying and locating mantle plumes*. In: Ernst, R. E. & Buchan, K. L. (Eds). Mantle Plumes: Their Identification through Time. Geological Society of America Special Paper, 352, 247–265.

Ernst, R. E. & Buchan, K. L. (2001b). *Large mafic magmatic events through time and links to mantle plume heads*. In: Ernst, R. E. & Buchan, K. L. (Eds). Mantle Plumes: Their identification through Time. Geological Society of America Special Paper, 352, 483–575.

Foley, S. (1992). Petrological characterization of the source components of potassic magmas: Geochemical and experimental constraints. *Lithos,* 28, 187-204. https://doi.org/10.1016/0024-4937(92)90006-K

Foley, S., & Peccerillo, A. (1992). Potassic and ultrapotassic magmas and their origin. *Lithos,* 28, 181-185. https://doi.org/10.1016/0024-4937(92)90005-J

Foley, S., Venturelli, G., Green, D. & Toscani, L. (1987). The ultrapotassic rocks: characteristics, classification, and constraints for petrogenetic models. *Earth-Science Reviews*, 24, 81-134. https://doi.org/10.1016/0012-8252(87)90001-8

Gibson, A., Thompson, R., Leat, P., Morrison, M., Hendry, G., Dicking, A. & Mitchell, J. (1992). Ultrapotassic magmas along the flanks of the Oligo-Miocene Rio Grande Rift, USA: Monitors of the zone of lithospheric mantle extension and thinning beneath a continental rift. *Journal of Petrology*, 34, 87-228. https://doi.org/10.1093/petrology/34.1.187

Girardi, V. A., Teixeira, W., Mazzucchelli, M. & Corrêa da Costa, P.C. (2013). Sr-Nd constraints and trace-elements geochemistry of selected Paleo and Mesoproterozoic mafic dikes and related intrusions from the South American Platform: Insights into their mantle sources and geodynamic implications. *Journal of South American Earth Sciences,* 41, 65–82. https://doi.org/10.1016/j.jsames.2012.09.006

Green, T. (1995). Significance of Nb/Ta as an indicator of geochemical processes in the crust-mantle system. *Chemical Geology*, 120, 347-359. https://doi.org/10.1016/0009-2541(94)00145-X

Gregoire, M., Moine B., O'Reilly S., Cottin J. & Giret, A. (2000). Trace element residence and partitioning in mantle xenoliths metasomatised by high alkaline silicate and carbonate-rich melts (Kerguelen Islands, Indian Ocean). *Journal of Petrology*, 41, 477–509. https://doi.org/10.1093/petrology/41.4.477

Gupta, A. (2015). *Origin of Potassium-rich Silica-deficient Igneous Rocks*. Springer, New Dehli, India, 536 pp.

Halls, H. C. & Fahrig, W. F. (1987). *Mafic dyke swarms*. Geological Association of Canada Special Paper, 34, 503 pp.

Halls, H. C., Campal, N., Davis, D. W. & Bossi, J. (2001). Magnetic studies and U–Pb geochronology of the Uruguayan dyke swarm, Rio de la Plata craton, Uruguay: paleomagnetic and economic implications. *Journal of South American Earth Sciences*, 14, 349 – 361. https://doi.org/10.1016/S0895-9811(01)00031-1

Hartmann, L. A., Pineyro, D., Bossi, J., Leite, J. A. D. & McNaughton, N. J. (2000). Zircon U–Pb SHRIMP dating of Paleoproterozoic Isla Mala granitic magmatism in the Rio de la Plata Craton, Uruguay. *Journal of South American Earth Sciences*,13, 105–113. DOI:10.1016/S0895-9811(00)00018-3

Hartmann, L. A., Campal, N., Santos, J. O. S., McNaughton, N. J., Bossi, J., Schipilov, A. & Lafon, J. M. (2001). Archean crust in the Rio de la Plata Craton, Uruguay - SHRIMP U–Pb zircon reconnaissance geochronology. *Journal of South American Earth Sciences,* 14, 557 – 570. https://doi.org/10.1016/S0895-9811(01)00055-4

Iacumin, M., Piccirillo, E. M., Girardi, V. A. V., Teixeira, W., Bellieni, G., Echeveste, H., Fernandez, R., Pinese, J. P. P. & Ribot, A. (2001). Early Proterozoic calc-alkaline and middle Proterozoic tholeiitic dike swarms from central-eastern Argentina: petrology, geochemistry, Sr–Nd isotopes and tectonic implications. *Journal of Petrology*, 42, 2109–2143. https://doi.org/10.1093/petrology/42.11.2109

Ionov, D., Griffin, W. & O'Reilly, S. (1997). Volatile- bearing minerals and lithophile trace elements in the upper mantle. *Chemical Geology*, 141, 153 - 184. https://doi.org/10.1016/S0009-2541(97)00061-2

Irving, T & Baragar, W. (1971). A guide to the chemical classification of the common volcanic rocks. *Journal of Earth Sciences*, 8, 523 - 548. https://doi.org/10.1139/e71-055

Le Bas, M., Le Maitre, R., Streckeisen, A., Zanettin, B. & IUGS Subcommission on the Systematics of Igneous Rocks (1986). A Chemical Classification of Volcanic Rocks Based on the Total Alkali-Silica Diagram. *Journal of Petrology*, 27(3), 745-750. https://doi.org/10.1093/petrology/27.3.745

Le Maitre, R. W., Streckeisen, A., Zanettin, B., Le Bas, M. J., Bonin, B., Bateman, P., Bellieni, G., Dudek, A., Efremova, S., Keller, J., Lameyere, J., Sabine, P. A., Schmid, R., Sørensen, H., & Woolley, A. R. (2002). *Igneous rocks: A Classification and Glossary of Terms*. Cambridge University Press, Cambridge, UK, 236 pp.

Loyd, F., Arima, M. & Edgar, A. (1985). Partial melting of a phlogopite cliopyroxenite nodule from south-west Uganda: an experimental

study bearing on the origin of highly potassic continental rift volcanics. *Contributions to Mineralogy and Petrology*, 91, 321-329. DOI: 10.1007/BF00374688

Lustrino, M., Melluso, L., Brotzu, P., Gomes, C., Morbidelli, L., Muzio, R., Ruberti, E., & Tassinari, C. (2005). Petrogenesis of the Early Cretaceous Valle Chico igneous complex (SE Uruguay): relationships with Paraná-Etendeka felsic rocks. *Lithos,* 82, 407-434. https://doi.org/10.1016/j.lithos.2004.07.004

Mahoney, J., Graham, D., Christie, D., Johnson, K., Hall, S., & Vonderhaar, D. (2002). Between a Hotspot and a Cold Spot: Isotopic Variation in the Southeast Indian Ridge Asthenosphere, 86°E–118°E. *Journal of Petrology*, 43(7), 1155-1176. https://doi.org/10.1093/petrology/43.7.1155

Marchese, H.G. & Di Paola, E. (1975). Miogeosinclinal Tandil. *Revista de la Asociación Geológica Argentina*, 30(2), 161-179.

Martino, N. (2017). *Estudio petrológico de diques lamprófidos en el sector sur del terreno Piedra Alta*. Graduation Thesis, Facultad de Ciencias, Universidad de la República, Montevideo, Uruguay, 115 pp.

Masquelin, E., Gutierrez, L., & Sienra, M. (2003). *Análisis estructural y cinemático de la Formación Montevideo*. VI Congreso Uruguayo de Geología, Montevideo, Uruguay, Actas, CD-ROM.

Mazzucchelli, M., Rivalenti, G., Piccirillo, E., Girardi, V. A. V., & Civetta, L. (1995). Petrology of the Proterozoic mafic dike swarms of Uruguay and constraints on their mantle source composition. *Precambrian Research*, 74, 177-194. https://doi.org/10.1016/0301-9268(95)00014-V

Mitchell, R. H. (1994). The lamprophyre facies. *Mineralogy and Petrology*, 51, 137-146. https://doi.org/10.1007/BF01159724

Mitchell, R. H. and Bergman, S.C. (1991). *Petrology of Lamproites*. Plenum Press, New York, USA, 447 pp.

Oyhantçabal, P., Spoturno, J., Aubet, N., Cazaux, S. & Huelmo, S. (2002). *La Formación Montevideo y los granito-neises asociados*. II Taller del Precámbrico del Uruguay. Montevideo, Uruguay, Actas, 11-17.

Oyhantçabal, P., Spoturno, J., Aubet, N., Cazaux, S. & Huelmo, S. (2003). Proterozoico del suroeste del Uruguay: nueva propuesta estratigráfica para la Formación Montevideo y el magmatismo asociado. *Revista Sociedad Uruguaya de Geología, Publicación Especial*, 1, 38-48.

Oyhantçabal, P., Siegesmund, S. & Wemmer, K. (2011). The Río de la Plata Craton: a review of units, boundaries, ages and isotopic signature. *International Journal of Earth Sciences,* 100, 201 – 220. https://doi.org/10.1007/s00531-010-0580-8

Pankhurst, R. J., Ramos, A. & Linares, E. (2003). Antiquity and evolution of the Río de la Plata craton in Tandilia, southern Buenos Aires province, Argentina. *Journal of South American Earth Sciences*, 16, 5–13.

Pascale, A. (2013). *Petrografía y geoquímica de las Anfibolitas de Formación Montevideo y los Ortoneises Asociados*. Graduation Thesis, Facultad de Ciencias, Universidad de la República, Montevideo, Uruguay, 130pp.

Pascale, A., & Oyhantçabal, P. (2010). *Estudio petrográfico-estructural de un afloramiento del Basamento Cristalino de Montevideo*. VI Congreso Uruguayo de Geología, Montevideo, Uruguay, Actas CD-ROM.

Peel, E. & Preciozzi, F. (2006). *Geochronologic synthesis of the Piedra Alta Terrane, Uruguay*. V South American Symposium on Isotope Geology, Punta del Este, Uruguay, Abstracts, 234-237.

Phillpotts, A. (1990). *Principles of Igneous and Metamorphic Petrology*. Prentice Hall. Englewood Cliffs, New Jersey, 498 pp.

Plá Cid, J., Campos, C., Nardi, L. & Florisbal, L. (2011). Petrology of Gameleira potassic lamprophyres, São Francisco Craton. *Anais da Academia Brasileira de Ciências,* 84(2), 377-398. https://doi.org/10.1590/S0001-37652012005000030

Preciozzi, F., Spoturno, J., & Heinzen, W. (1979). *Carta geo-estructural del Uruguay a escala 1/2.000.000*. Instituto Geológico Ing. Eduardo Terra Arocena, Montevideo, Uruguay, 42 pp.

Preciozzi, F., Basei, M. A. & Masquelin, E. (1999). *New geochronological data from the Piedra Alta Terrane (Río de la Plata Craton)*. II South American Symposium on Isotope Geology, Córdoba, Argentina, Abstracts, 341-344.

Quartino, B. J. & Villar Fabre, J. F. (1967). Geología y petrología del basamento de Tandil y Barker (provincia de Buenos Aires) a la luz del estudio de las localidades críticas. Revista de la Asociación Geológica Argentina, 22(3), 223-251.

Rapela, C. W., Pankhurst, R. J., Casquet, C., Fanning, C. M., Baldo, E. G., González-Casado, J. M., Galindo, C. & Dahlquist, J. (2007). The Rio de la Plata Craton and the assembly of SW Gondwana. Earth Sciences Review, 83, 49–82. https://doi.org/10.1016/j.earscirev.2007.03.004

Rapela, C. W., Fanning, C. M., Casquet, C., Pankhurst, R. J., Spalletti, L., Poiré, D. & Baldo, E. G. (2011). The Rio de la Plata Craton and the adjoining Pan-African/Brasiliano Terranes: Their origins and incorporation into South-West Gondwana. *Gondwana Research,* 20(4), 673–690. https://doi.org/10.1016/j.gr.2011.05.001

Reed, J. (2005). *Electron Microprobe analysis and scanning electron microscopy in geology*. Cambridge University Press, Cambridge, UK, 216 pp.

Rock, N. M. S. (1987). The nature and origin of lamprophyres: an overview. *Geological Society, London, Special Publications*, 30, 191–226. https://doi.org/10.1144/GSL.SP.1987.030.01.09

Rock, N.M.S. (1991). *Lamprophyres*. Blackie & Son (Editors), Glasgow – London-New York, 285 pp.

Rhodes, J. (1981). *Characteristics of primary basaltic magmas*. In: Basaltic Volcanism on the Terrestrial Planets, Pergamon, New York, USA, 409 - 432.

Sánchez Bettucci, L., Peel, E. & Oyhantcabal, P. (2010). Precambrian geotectonic units of the Río de La Plata craton. *International Geology Review,* 52(1), 32–50. DOI:10.1080/00206810903211104

Severin, K. P. (2004). *Energy Dispersive Spectrometry of Common Rock Forming Minerals*. Department of Geology and Geophysics, University of Alaska Fairbanks, U.S.A, 228 pp.

Spell, T. L. & McDougall, I. (2003). Characterization and calibration of 40Ar/39Ar dating standards. *Chemical Geology*, 198, 189 - 211. https://doi.org/10.1016/S0009-2541(03)00005-6

Spoturno, J. J., Oyhantçabal, P., Goso, C., Aubet, N., Cazaux, S. & Morales, E. (2004). Mapa geológico y recursos minerales del Departamento de Montevideo, escala 1/50.000. DINAMIGE – Facultad de Ciencias (Editors), Montevideo, Uruguay, CD.

Staudacher, T. H., Jessberger, E. K., Dorflinger, D. & Kiko, J. (1978). A refined ultrahigh-vacuum furnace for rare gas analysis. *Journal of Physics Earth Sciences: scientific instruments*, 2(8), 781–784.

Sun, S. & McDonough, W. F. (1989). Chemical and isotopic systematics of oceanic basalts: implications for mantle composition and processes. *Geological Society London, Special Publications,* 42, 313-345. https://doi.org/10.1144/GSL.SP.1989.042.01.19

Tappe, S., Foley, S., Jenner, G. & Kjarsgaard, B. (2005). Integrating Ultramafic Lamprophyres into the IUGS classification of igneous rocks: rationale and implications. *Journal of Petrology*, 46(9), 1893-1900. https://doi.org/10.1093/petrology/egi039

Teixeira, W., Renne, P. R., Bossi, J., Campal, N. & D'Agrella-Filho, M. S. (1999). [40]Ar–[39]Ar and Rb–Sr geochronology of the Uruguayan dike swarm, Rio de la Plata Craton and implications for Proterozoic intraplate activity in western Gondwana. Precambrian Research, 93, 153–180. https://doi.org/10.1016/S0301-9268(98)00087-4

Teixeira, W., Pinese, J. P. P., Iacumin, M., Girardi, V. A. V., Piccirillo, E. M., Echevest, E. H., Ribot, A., Fernandez, R., Renne, P. R. & Heaman, L. M. (2002). Calc-alkaline and tholeitic dike swarms of Tandilia, Rio de la Plata craton, Argentina: U–Pb, Sm–Nd, Rb–Sr and 40Ar/39Ar data provide new clues for intraplate rifting shortly after the Trans - Amazonian orogeny. *Precambrian Research,* 119, 329–353. https://doi.org/10.1016/S0301-9268(02)00128-6

Teixeira, W., D´Agrella Filho, M. S., Ernst, R. E., Girardi, V. A., Mazzucchelli, M. & Bettencourt, J.S. (2013). U–Pb (ID-TIMS) baddeleyite ages and paleomagnetism of 1.79 and 1.59 Ga tholeiitic dyke swarms, and position of the Rio de la Plata Craton within the Columbia supercontinent. *Lithos*, 174, 157–174. https://doi.org/10.1016/j.lithos.2012.09.006

Turner, S., Arnaud, N., Liu, J., Rogers, N., Hawkesworth, C., Harris, N., Kelley, S., Van Calsteren, P. & Deng, W. (1996). Post collision shoshonitic volcanism on the Tibetan plateau: implications for convective thinning

of the lithosphere and the source of ocean island basalts. *Journal of Petrology*, 37, 45–71. https://doi.org/10.1093/petrology/37.1.45

Wallace, P. & Carmichael, I. (1989). Minettes lavas and associated leucitites from the western front of the Mexican volcanic belt: petrology, chemistry and origin. *Contributions to Mineralogy and Petrology*, 103, 470-492. https://doi.org/10.1007/BF01041754

Whalen, J., Currie, K. & Chappel, B. (1987). A-type granites: geochemical characteristics, discrimination and petrogenesis. *Contributions to Mineralogy and Petrology*, 95, 407-419. https://doi.org/10.1007/BF00402202

Walther, K. (1935). *La estructura geológica de los alrededores de Montevideo. Anales del Museo de Historia Natural de Montevideo*. 2da serie, 4 (7), Montevideo, Uruguay, 164-179.

Walther, K. (1948). *El basamento cristalino de Montevideo*. Instituto Geológico del Uruguay, Boletín N.º 33, Montevideo, Uruguay, 198 pp.

Wendt, I. & Carl, C. (1991). The statistical distribution of the mean squared weighted deviation. *Chemical Geology*, 86, 275-285. https://doi.org/10.1016/0168-9622(91)90010-T

Winchester, J. A. & Floyd, P. A. (1977). Geochemical discrimination of different magma series and their differentiation products using immobile elements. *Chemical Geology,* 20, 325-343. https://doi.org/10.1016/0009-2541(77)90057-2